ISSN 1018-5593

European Commission

Global change

Proceedings of the first Demetra meeting held at Chianciano Terme, Italy from 28 to 31 October 1991

EUR 15158 EN

SELECTING COMPONENTS OF A GREENHOUSE-GAS FINGERPRINT

Benjamin D. Santer, Ulrich Cubasch, Klaus Hasselmann, Wolfgang Brüggemann, Heinke Höck, Ernst Maier-Reimer, and Uwe Mikolajewicz

Max-Planck-Institut für Meteorologie
Bundesstrasse, 55
D-W - 2 Hamburg 13

ABSTRACT

Results from a control integration and time-dependent greenhouse warming experiments performed with a coupled ocean-atmosphere model are analysed in terms of their signal-to-noise properties. The aim is to identify components of a multivariate "fingerprint" vector which may be useful for detecting greenhouse-gas-induced climate change. The three 100-year experiments analysed here simulate the response of the climate system to a step-function doubling of CO_2 and to the time-dependent greenhouse gas increases specified in Scenarios A ("Business as Usual") and D ("Draconian Measures") of the Intergovernmental Panel on Climate Change (IPCC).

The pattern correlation between the dominant EOF of the control run and the response experiments is used to measure the orthogonality of signal and noise patterns. For signal detection, the most favorable orthogonality relationships are obtained for surface air temperature, precipitable water, and zonally-averaged vertical temperature changes (stratospheric cooling and tropospheric warming). The EOF 1 pattern of sea level pressure in the Scenario A and $2xCO_2$ experiments is similar to the pattern of the dominant noise EOF. Between - variable pattern correlations indicate that near surface temperature and precipitable water provide non-overlapping information about the predicted signal.

In order to obtain estimates of the variance of linear trends on timescales of up to 100 years, we use results from a 3,800-year "natural variability"

integration performed with an uncoupled ocean model. This information is then used to assess the significance of linear trends in principal component (PC) time series from the control and Scenario A experiments. For surface temperature, the overall linear trend in PC 1 of Scenario A is over three times larger than the variance of 100-year trends estimated from the natural variability experiment. Appropriate paleoclimate data and long ($\geq$ 500 years) natural variability experiments with fully coupled ocean-atmosphere models are required in order to confirm these results.

1. INTRODUCTION

Recently, considerable attention has been devoted to the problem of detecting the climatic signature of the enhanced greenhouse effect (Wigley and Barnett, 1990). It has been proposed that the chances of detecting an enhanced greenhouse effect in the observations would be improved by the use of a multivariate "fingerprint" (Madden and Ramanathan, 1980; MacCracken and Moses, 1982). At least five criteria have been proposed for selecting the components of such a fingerprint vector (Barnett and Schlesinger, 1987; Wigley and Barnett, 1990; Barnett, 1991; Santer et al., 1992):

1. Each individual component should have high signal-to-noise ratios in the model-predicted data.
2. The "fingerprint" vector should not differ from model to model.
3. The "fingerprint" vector should be easily distinguished from (i.e., orthogonal to) the signals due to forcing factors other than greenhouse gases and from the noise of natural internally-generated variability on the 10-100 year timescale relevant to the detection of the greenhouse effect.
4. Each component of the "fingerprint" vector should provide information which does not strongly overlap with the information of other components.
5. Suitable observational data should exist. Because it is the 10-100 year timescale that is of concern, long data records are needed.

Here, we examine output from time-dependent experiments performed with a coupled ocean-atmosphere model according to the signal-to-noise, orthogonality, and uniqueness of information criteria (1,3,4). The aim is to demonstrate techniques for identifying potentially useful components of a greenhouse gas "fingerprint".

Signal-to-noise (S/N) and orthogonality properties can be defined in a number of different ways. In the context of greenhouse gas response experiments, three aspects have been examined:

1. Overall magnitude; e.g., some measure of the overall change in mean (response minus control) relative to the temporal variance of the control or the (pooled) variance of control and response (Wigley and Jones, 1981; Barnett and Schlesinger, 1987; Barnett et al., 1991; Santer et al., 1991).
2. The similarity of signal and noise spatial patterns (Barnett and Schlesinger, 1987; Barnett et al., 1991; Mikolajewicz et al., 1991).
3. The relationship between the magnitude of a trend in a time-evolving signal and the variance of trends (on the time scale appropriate to the signal) in a long control run (Mikolajewicz et al., 1991).

Previous studies have focussed on items (1) and (2). As more time-dependent greenhouse gas experiments are performed, it will become increasingly important to consider (3) and explicitly include the time dimension in estimating S/N properties. The problem is to determine whether the trend in a time-dependent response experiment is large relative to the trends which could occur due to internally-generated natural variability.

Since any climate signal due to the enhanced greenhouse effect evolves on the decadal to century timescales, we are primarily interested in analysing the noise on similar timescales. Here, we use results from a 3,800-year "natural variability" integration performed with an uncoupled ocean model (Mikolajewicz and Maier-Reimer, 1990) in order to estimate the variance of linear trends on timescales of up to 100 years. This information is then used to assess the S/N properties of principal component (PC) time series from the Scenario A experiment.

It should be stressed that there are (and will continue to be) model-dependent ucnertainties in defining an enhanced greenhouse effect, signal, and in determining the magnitude and spatial structure of low frequency internally-generated natural variability. The focus of this study, therefore, is on methodological aspects, and further experiments are necessary in order to confirm the results presented here.

2. THE COUPLED MODEL

The model which was used for performing the time-dependent integrations described below consists of an atmospheric GCM (ECHAM1) coupled synchronously to an ocean GCM (LSG). ECHAM1 is a low resolution (T21; 19 vertical layers) version of the spectral model developed at the European Centre for Medium Range Weather Forecasts (ECMWF). It has been extensively modified for climate purposes in Hamburg (Roeckner et al., 1989), and has been used for a number of different sensitivity experiments (Cess et al., 1989; Lautenschlager and Herterich, 1990).

The LSG (Large Scale Geostrophic) ocean GCM developed by Maier-Reimer and Hasselmann (1987) is based on a numerical formulation of the primitive equations appropriate for large scale geostrophic motion. It has 11 vertical levels and a horizontal resolution of 3.5° x 3.5°. A detailed description of the model physics and control run performance is given by Maier-Reimer et al. (1991). The LSG model has been used in a variety of ocean circulation studies (Maier-Reimer and Mikolajewicz, 1989; Mikolajewicz and Maier-Reimer, 1990; Mikolajewicz et al., 1990).

A full description of the coupling procedure and flux correction scheme (Sausen et al., 1988) is given in Cubasch et al. (1991), together with information on the fidelity with which the coupled model reproduces important features of the observed climate.

3. CONTROL AND GREENHOUSE WARMING SIMULATIONS

The recent report of Working Group 1 of the Intergovernmental Panel on Climate Change (IPCC) presents four scenarios of future changes in greenhouse gas concentrations, ranging from unrestriced emissions in Scenario A ("Business as Usual") to severe restriction of greenhouse gas emissions after the year 2000 in Scenario D ("Draconian Measures"). Scenarios A and D were used to force the coupled model in two separate 100-year experiments. In the third greenhouse warming experiment, the response of the coupled model to an instantaneous doubling of equivalent atmospheric CO_2 concentration was considered. For reference, a 100-year control run was performed with fixed equivalent CO_2 concentration.

A full description of the design of the control run and greenhouse warming experiments is given in Cubasch et al. (1991), together with a brief analysis of the evolution of the surface air temperature signal.

4. EVOLUTION OF SURFACE AIR TEMPERATURE IN CONTROL RUN

The global mean annually-averaged near surface air temperature drifts by less than 0.4° K during the 100-year integration (Figure 1). This quasi-stationarity with respect to the global mean masks large positivie and negative changes in the spatial distribution of temperature, with high latitude cooling in the Northern Hemisphere and warming in the Southern Hemisphere. The zonally averaged changes in near surface temperature (relative to the average of the first 10 years of the control run) are coherent in time and space (Figure 2). In the final decade of the control run there is strong cooling ($\approx$ 5°C) in the Arctic and warming in the Ross ($\approx$ 6°C) and Weddell ($\approx$ 4°C) Seas (Figure 3). The area-weighted r.m.s. of this anomaly field is 1.1°C.

Does this behaviour of the control run represent internally-generated natural variability of the coupled ocean-atmosphere system (on timescales of a century or longer), spurious drift, or some combination of drift and natural variability? This a key question if the results obtained here are to have any relevance for detection of a model-predicted greenhouse gas signal in the observed data.

Unfortunately, it is very difficult to discriminate between drift and natural variability without performing significantly longer integrations ($\geq$ 500 years) with the coupled model. Such experiments have not yet been conducted. Therefore, we cannot definitively answer the question of whether the control run changes are due to drift or natural variability. Here we briefly examine the evidence for each interpretation.

Some evidence for a natural variability interpretation can be gained by comparing our results with data from a 3,800-year integration with the LSG ocean model (Mikolajewicz and Maier-Reimer, 1990; henceforth MM), in which the ocean was forced by white noise superimposed on the climatological fresh water fluxes. This uncoupled experiment yielded typically red variance spectra for a variety of ocean circulation indices (e.g. heat transport, streamfunction, ice volume, etc.), with power increasing monotonically towards low frequencies for time scales up to several centuries. The variability displayed by the coupled model is consistent with these results. There is also some agreement in the spatial pattern of variability: Both coupled and uncoupled experiments showed large variability in the vicinity of the Antarctic Circumpolar Current, a relatively sensitive region of the ocean circulation. However, in view of the idealized nature of the uncoupled experiment (surface temperature is essentially prescribed), we cannot determine whether the spatial structure of the temperature changes in Figures 2 and 3 is in fact consistent with the dominant natural

variability patterns implied in the MM experiment.

Further insights into the nature of the non-stationarity demonstrated by the control run can be gained by comparing the spatial patterns of the control run anomalies and the flux correction fields (not shown). There is close agreement between the location of the large, positive SST anomalies in the Ross and Weddell Seas in the control run and the location of the largest heat flux corrections. This suggests that some of the non-stationarity in control run SST may be attributable to incomplete drift compensation by the flux correction, at least at high latitudes in the Southern Hemisphere. In the Northern Hemisphere, however, the alternating warm and cool episodes (Figure 2) are difficult to explain by drift alone, since the flux corrections applied are invariant from year to year.

In the presence of substantial climate drift and/or natural variability, the evolution of the signal and its S/N properties can be sensitivie to the way in which the signal is defined. Here, we regard the non-stationarity of the control run as inherent natural variability of the coupled model. Assuming that the natural variability in the control run and the response experiments are uncorrelated, we define the time-dependent climate response in the greenhouse warming simulations as the deviation with respect to the average of the first 10 years of the control run (see Cubasch et al., 1991, for an alternative definition).

5. SIGNAL-TO-NOISE ORTHOGONALITY PROPERTIES

Cubasch et al. (1991) used the pattern correlation between the first EOFs of the control run and the response experiments in order to measure the orthogonality of signal and noise patterns. This was done for surface air temperature only. Here, we consider a number of other variables (Table 1). A high pattern correlation indicates close correspondence between signal and noise patterns and poor orthogonality properties. For signal detection, the most favorable orthogonality relationships are obtained for surface air temperature (Figures 4a,b) and vertically-integrated precipitable water. Sea-level pressure shows the least favorable orthogonality properties, a result which agrees well with other studies (Barnett et al., 1991). For surface air temperature, the pattern correlation between EOF 1 of the control run and EOF 1 Scenario A is only 0.43 (This is associated mainly with the strong variability at high southern latitudes). This indicates that the dominant greenhouse warming pattern of the response experiment cannot have been strongly affected, in the space-time average, by a possible common spurious drift or natural variability signal. This conclusion is supported by the principal component (PC) time series shown in Figure 5. To generate these time series

we projected the signals of the control run and all three experiments (as defined in Section 4) onto EOF 1 of Scenario A. The coefficient of the Scenario A EOF 1 pattern in the control run is close to zero. This shows that the dominant greenhouse warming signal in Scenario A can be clearly distinguished from the model's natural variability and/or drift.

A strong vertical temperature contrast (stratospheric cooling and tropospheric warming) is a common feature of the greenhouse-gas signals simulated in a number of different model experiments (e.g. Schlesinger and Mitchell, 1987; Cubasch et al., 1991). Recently, Karoly (1987, 1989) has compared such signals with observations, and suggests that vertical temperature contrasts could be useful for detecting greenhouse-gas-induced climatic change. However, as Liu and Schuurmanns (1990) and Wigley and Barnett (1990) have pointed out, this characteristic signal may resemble the observed pattern of vertical temperature changes associated with low-frequency internally-generated natural variability. Our results suggest that the structure of the dominant control run EOF for vertical temperature changes is only weakly correlated (0.46) with the EOF 1 pattern of Scenario A (Table 1 and Figures 6a,b). There is, however, some correspondance of signal and noise patterns in the tropical troposphere and stratosphere, which requires further investigation.

As noted by Barnett and Schlesinger (1987), each component of a multivariate detection vector should provide unique information. In order to test how well different variables fulfil this condition, we computed the between-variable pattern correlations for the first EOF of Scenario A (Table 2). The correlation between EOF 1 of surface air temperature and vertically-integrated precipitable water (which both showed favorable orthogonality properties; see Table 1) is only 0.23, indicating that these variables provide non-overlapping information about the predicted signal. This low correlation is due to the fact theat EOF 1 of vertically-integrated precipitable water (not shown) has a strong tropical component and does not show pronounced land/sea contrast (c.f. Figure 4a). This suggests that both surface air temperature and precipitable water would be useful components of a multivariate detection vector.

6. SPECTRAL ESTIMATES OF SIGNAL-TO-NOISE BEHAVIOUR

How do we assess whether the trends simulated in the three transient experiments described above are significant relative to the noise of the model's own internally-generated natural variability? This question has not been addressed in previous studies involving time-dependent forcing of coupled ocean-atmosphere models. One of the difficulties involved in

Table 1: **Spatial correlation between EOF 1 of the control run and EOF 1 of the Scenario A experiment for a number of different variables**

ORTHOGONALITY OF SIGNAL AND NOISE

No.	VARIABLE	Correlation	EV. EOF1 CTL (%)	EV. EOF1 SZA (%)
1	2 m Temperature	0.43	52.5	84.1
2	Vertical Temperature	0.46	61.4	97.6
3	Precipitable Water	0.50	27.7	89.5
4	Precipitation Rate	0.55	12.8	17.3
5	Total Cloud Cover	0.57	16.1	22.4
6	10 m U-Velocity	0.67	17.4	28.4
7	10 m V-Velocity	0.69	20.1	25.9
8	Sea Level Pressure	0.82	27.7	36.9

Table 2: **Between-variable spatial correlation for EOF 1 of Scenario A. Correlations indicate the variables which provide overlapping information**

BETWEEN VARIABLE PATTERN CORRELATIONS

VARIABLE	TEMP	PWAT	PREC	MSLP	CLDS	UVEL	VVEL
TEMP[a]	1.00	0.23	0.04	0.18	0.29	0.16	0.21
PWAT[b]		1.00	0.17	0.37	0.02	0.14	0.05
PREC[c]			1.00	0.13	0.52	0.20	0.11
MSLP[d]				1.00	0.39	0.27	0.28
CLDS[e]					1.00	0.14	0.22
UVEL[f]						1.00	0.21
VVEL[g]							1.00

[a] TEMP: 2 m temperature
[b] PWAT: Vertically-integrated precipitable water
[c] PREC: Total precipitation rate
[d] MSLP: Mean sea level pressure
[e] CLDS: Total cloud cover
[f] UVEL: 10 m u-velocity
[g] VVEL: 10 m v-velocity

answering this question is that (due to computational restrictions) state-of-the-art coupled models have been integrated for only $\leq$ 100 years (Stouffer et al., 1989; Cubasch et al., 1991). From a single 100-year control integration, a reliable estimate of the magnitude of century timescale natural variability cannot be derived. It is precisely the decadal to century timescale, however, that is important for the detection of a slowly-evolving greenhouse gas signal.

One method of estimating the magnitude of natural variability on the century timescale would be to use long paleoclimate records with high temporal resolution, such as the 1400-year tree ring chronology for Scandinavia developed by Briffa et al. (1990). However, such reconstructions generally explain no more than 50 % of the variance associated with temperature. Further, we are interested here in determining the significance of 100-year trends derived from global data, such as the principal component time series shown in Figure 5. It may be inappropriate to use low-frequency variance estimates obtained from regionally-specific observed data for this specific purpose.

Long experiments ($\geq$ 1000 years) with uncoupled models provide a further source of information concerning century timescale natural variability. Here, we use results from the 3,800-year "natural variability" experiment performed by MM in order to estimate the variance of linear trends onthe century timescale. The disadvantage of this approach is that (in the absence of results from long experiments with coupled ocean-atmosphere models) we do not know whether the low-frequency variance information derived from the ocean model alone is a good analogue for the results from a long experiment with a fully-coupled model. The advantage (relative to paleoclimate records) is that data from the 3,800-year natural variability experiment are available for the global ocean and have high temporal resolution.

6.1 Significance of Linear Trends

The significance of a trend can be determined in either the time domain or in the frequency domain (Bloomfield and Nychka, 1991). In both cases, the variance of the parameters describing the trend (the standard error) must be computed. Here, we use the approach outlined by Bloomfield and Nychka (1991) in order to compute the standard error, b, for linear trends on the 100-year timescale.

Ideally, it would have been desirable to subject the output of the MM natural variability experiment to the same statistical analysis which was applied to the transient CO_2 experiments (EOF analysis), and then to compute b for the principal component time series. This was not possible, since fields such as 2 m temperature in the transient CO_2 experiments are

effectively prescribed in the uncoupled MM experiment. Here, we derive a range of estimates for b using time series of annual averages for various ocean variables from the MM natural variability experiment. The time series are global and regional (NorthAtlantic, North Pacific, Antarctic) averages for ice coverage, heat flux, salinity, loss of potential energy by convective overturning, etc. Each time series is converted into anomaly form, normalized, and divided into chunks of 100 years in order to compute b. The standard error then provides non-dimensional information on the variance of linear trends (due to internally-generated natural variability alone) on the 100-year timescale. Normalization ensures that values of b are comparable for variables with different variances. The principal component time series from the transient CO_2 experiments (Figure 5) were also normalized in order to assess the significance of their linear trends.

Estimates of b from the MM natural variability experiment are shown in Figure 7. The largest values of b are for ice coverage and loss of potential energy by convective overturning in the North Atlantic and Antarctic, while the smallest values of b are for globally-averaged temperature and salinity in the fourth model layer. Values of b are consistently smaller for globally-averaged quantities than for averages over an ocean basin. The mean value of b for all 17 variables is 0.0104, with a standard deviation of 0.0028. Values of b are also given for the spatially-correlated white-noise freshwater flux which was used to force the LSG OGCM (variables 18-21 in Figure 7). As expected, these are smaller than the values for all output variables. Note that for surface air temperature, the overall linear trend in PC 1 of Scenario A is over three times larger than the mean value of b.

Table 3 shows the average linear trend per year, b_{LS},[1] in the (normalized) first principal component time series for the Scenario A experiment and the control integration. We assume that these trends are the signals of interest, and that the average value of b derived from the MM experiment[2] is representative of century timescale internally-generated variability. The raio b_{LS}/b is a measure of signal strength. For Scenario A, signal strength is largest for 2 m temperature and precipitable water and smallest for sea level pressure. This ranking of variables in terms of their temporal signal-to-noise behaviour is similar to the ranking in terms of spatial signal-to-noise characteristics (see Table 1).

---

[1] Fitted by least-squares regression.

[2] Excluding the values of b for the whith-noise forcing terms, i.e., variables 18-21 in Figure 7.

Table 3:

Linear trends for 100-year principal component time series. Results are from the Scenario A experiment and the control run and are for the first principal component time series only. Trends were determined by least squares regression (after normalization) and are expressed as the average trend per year. Numbers in brackets indicate the ratio between the linear trend and the average value of *b* (the variance of linear trends on timescales of 100 years) from the Mikolajewicz and Maier-Reimer (1990) natural variability experiment.

LINEAR TRENDS FOR PC TIME SERIES

No.	VARIABLE	SZA		CTL	
1	2 m Temperature	0.0340	(3.27)	0.0068	(0.65)
2	Precipitable Water	0.0339	(3.26)	0.0270	(2.60)
3	Precipitation Rate	0.0299	(2.88)	0.0070	(0.67)
4	Sea Level Pressure	0.0146	(1.40)	0.0002	(0.02)

7. CONCLUSIONS

The aim of this analysis was to identify components of a multivariate "fingerprint" which may be useful for detecting greenhouse-gas induced climate change. We used three different aspects in order to identify "useful" variables: orthogonality of signal and noise patterns, uniqueness of information provided, and the relationship between the magnitude of trends in the response experiments and the variance of linear trends on timescales of 100 years (b_{LS}/b). Surface air temperature and vertically-integrated precipitable water fulfil all three criteria. In contrast, the signal and noise patterns of SLP are similar.

These results suggest that surface temperature, vertical temperature contrasts and precipitable water would be good choices for a multivariate detection vector, while SLP would be a poor choice. Appropriate paleoclimate data and long ($\geq$ 500 years) natural variability experiments with fully coupled ocean-atmosphere models are required in order to corroborate these findings. Attempts should also be made in order to define an "optimum" greenhouse gas detection vector (Hasselmann, 1979), and to determine the characteristic fingerprints of other forcing mechanisms, such as solar variability and volcanic aerosols.

REFERENCES

Barnett, T.P. and Schlesinger, M.E., 1987: Detecting changes in global climate induced by greenhouse gases. Journal of Geophysical Research 92, 14,772-14, 780

Barnett, T.P., 1991: An attempt to detect the greenhouse-gas signal in a transient GCM simulation. In: Greenhouse-Gas-Induced Climatic Change: A Critical Appraisal of Simulations and Observations (Ed. M.E. Schlesinger), 559-568. Elsevier Science Publishers, Amsterdam

Barnett, T.P., Schlesinger, M.E. and Jiang, X., 1991: On greenhouse gas detection strategies. In: Greenhouse-Gas-Induced Climatic Change: A Critical Appraisal of Simulations and Observations (Ed. M.E. Schlesinger), 537-558. Elsevier Science Publishers, Amsterdam

Bloomfield, P. and Nychka, D., 1991: Climate spectra and detecting climate change. Submitted to Climatic Change

Briffa, K.R., Bartholin, T.S., Eckstein, D., Jones, P.D., Karlén, W., Schweingruber, F.H. and Zetterberg, P., 1990: A 1,400-year tree-ring record of summer temperatures in Scandinavia. Nature 346, 434-439

Cess, R.D., Potter, G.L., Blanchet, J.P., Boer, G.J., Ghan, S.J., Keihl, J.T., Le Treut, H., Li, Z.X., Liang, X.Z., Mitchell, J.F.B., Morcrette, J-J., Randall, D.A., Riches, M.R., Roeckner, E., Schlese, U., Slingo, A., Taylor, K.E., Washington, W.M., Wetherald R.T. and Yagai, I., 1989: Interpretation of cloud climate feedback as produced by 14 atmospheric general circulation models. Science 245, 513-516

Cubasch, U., Hasselmann, K., Höck, H., Maier-Reimer, E., Mikolajewicz, U., Santer, B.D. and Sausen, R., 1991: Time-dependent greenhouse warming computations with a coupled ocean-atmosphere model. Max-Planck-Institut für Meteorologie Report No. 67, Hamburg, FRG, 18 pp

Hasselmann, K., 1979: On the signal-to-noise problem in atmospheric response studies. In: Meteorology of Tropical Oceans (Ed. D.B. Shaw). Royal Meteorological Society, 251-259

Karoly, D.J., 1987: Southern Hemisphere temperature trends: A possible greenhouse gas effect? Geophysical Research Letters 14, 1139-1141

Karoly, D.J., 1989: Northern Hemisphere temperature trends: A possible greenhouse gas effect? Geophysical Research Letters 16, 465-468

Lautenschlager, M. and Herterich, K., 1990: Atmospheric response to ice age conditions -

climatology near the earth's surface. Journal of Geophysical Research 95, 22,547-22,557

Liu, Q. and Schuurmaans, C.J.E., 1990: The correlation of tropospheric and stratospheric temperatures and its effect on the detection of climate changes. Geophysical Research Letters 17, 1085-1088

MacCracken, M.C. and Moses, H., 1982: The first detection of carbon dioxide effects: Workshop Summary, 8-10 June 1981, Harpers Ferry, West Virginia. Bulletin of the American Meteorological Society 63, 1164-1178

Madden, R.A. and Ramanathan, V., 1980: Detecting climate change due to increasing carbon dioxide. Science 209, 763-768

Maier-Reimer, E. and Hasselmann, K., 1987: Transport and storage of CO_2 in the ocean - an inorganic ocean-circulation carbon cycle model. Climate Dynamics 2, 63-90

Maier-Reimer, E. and Mikolajewicz, U., 1989: Experiments with an OGCM on the cause of the Younger Dryas. In: Oceanography 1988 (Eds. A. Ayala-Castanares, W. Wooster and A. Yanez-Arancibia). UNAM Press, Mexico, pp 87-100

Mikolajewicz, U. and Maier-Reimer, E., 1990: Internal secular variability in an ocean general circulation model. Climate Dynamics 4, 145-156

Mikolajewicz, U., Maier-Reimer, E. and Barnett, T.P., 1991: Acoustic detection of greenhouse-induced climate changes in the presence of natural variability. Max-Planck-Institut für Meteorologie Report No. 69, Hamburg, FRG, 37 pp

Mikolajewicz, U., Santer, B.D. and Maier-Reimer, E., 1990: Ocean response to greenhouse warming. Nature 345, 589-593

Roeckner, E., Dümenil, L., Kirk, E., Lunkeit, F., Ponater, M., Rockel, B., Sausen, R. and Schlese, U., 1989: The Hamburg version of the ECMWF model (ECHAM). In: Research Activities in Atmospheric and Oceanic Modelling. (Ed. G.F. Boer). CAS/JSC Working Group on Numerical Experimentation 13:7.1-7.4, WMO Technical Document 322, Geneva

Santer, B.D., Wigley, T.M.L., Schlesinger, M.E. and Jones, P.D., 1991: Multivariate methods for the detection of greenhouse-gas-induced climate change. In: Greenhouse-Gas-Induced Climatic Change: A Critical Appraisal of Simulations and Observations (Ed. M.E. Schlesinger), 511-536. Elsevier Science Publishers, Amsterdam

Santer, B.D., Wigley, T.M.L. and Jones, P.D., 1992: Towards the detection of an enhanced greenhouse effect fingerprint. (In preparation)

Sausen, R., Barthel, K. and Hasselmann, K., 1988: Coupled ocean-atmosphere models with flux corrections. Climate Dynamics 2, 154-163

Schlesinger, M.E. and Mitchell, J.F.B., 1987: Climate model simulations of the equilibrium climatic response to increased carbon dioxide. Reviews of Geophysics 25, 760-798

Stouffer, R.J., Manabe, S. and Bryan, K., 1989: Interhemispheric asymmetry in climate reponse to a gradual increase of atmospheric CO_2. Nature 342, 660-662

Wigley, T.M.L. and Barnett, T.P., 1990: Detection of the greenhouse effect in the observations. In: Climate Change. The IPCC Scientific Assessment (Eds. J.T. Houghton, G.J. Jenkins and J.J. Ephraums). Cambridge University Press, Cambridge, pp 239-256

Wigley, T.M.L. and Jones, P.D., 1981: Detecting CO_2-induced climatic change. Nature 292, 205-208

FIGURE 1: Time evolution of the global mean surface air temperature change for the three greenhouse warming simulations, the control experiment and the IPCC "best estimates".

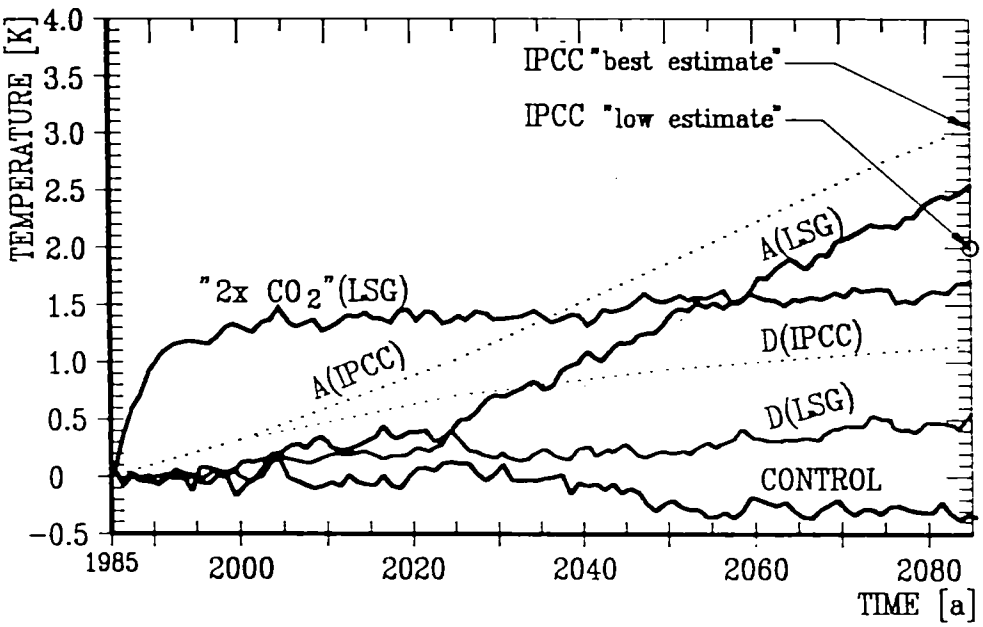

FIGURE 2: Time evolution of zonally-averaged changes in annual mean surface air temperature in the 100-year control integration. Changes are expressed relative to the smoothed initial state (average over years 1-10) of the control run.

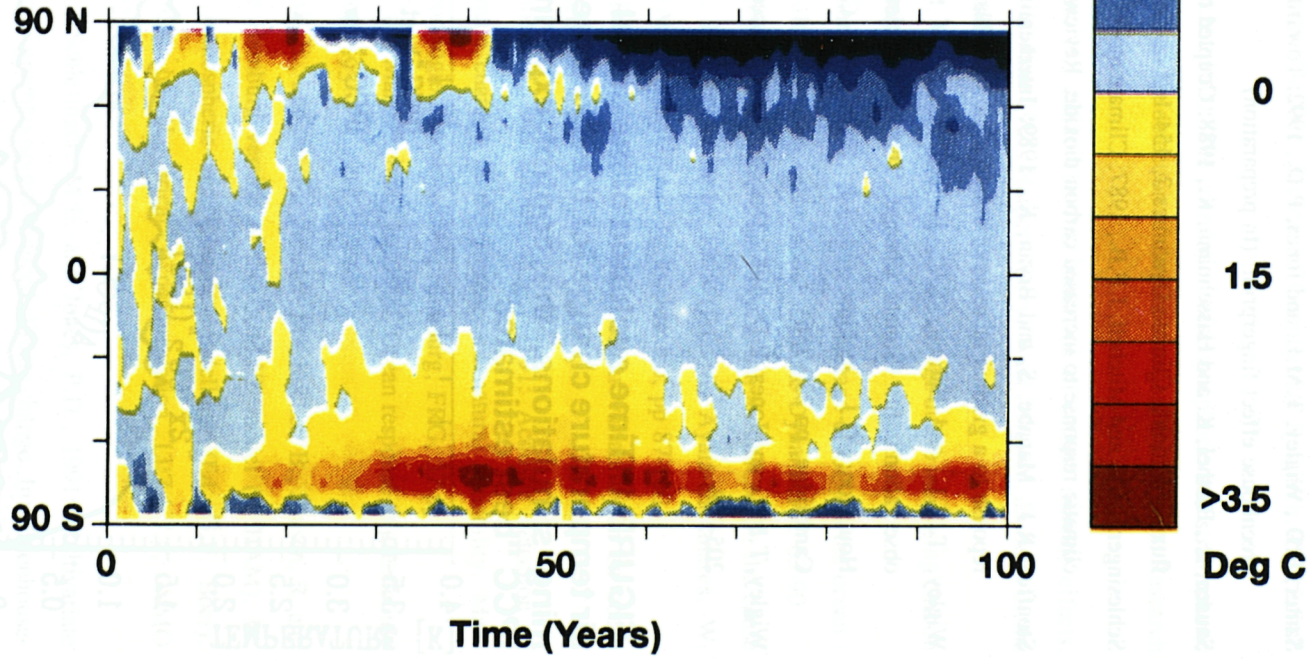

FIGURE 3: Geographical distribution of the changes in annually-averaged surface air temperature for the final decade (years 91-100) of the control integration. Changes are expressed relative to the smoothed initial state (average over years 1-10) of the control.

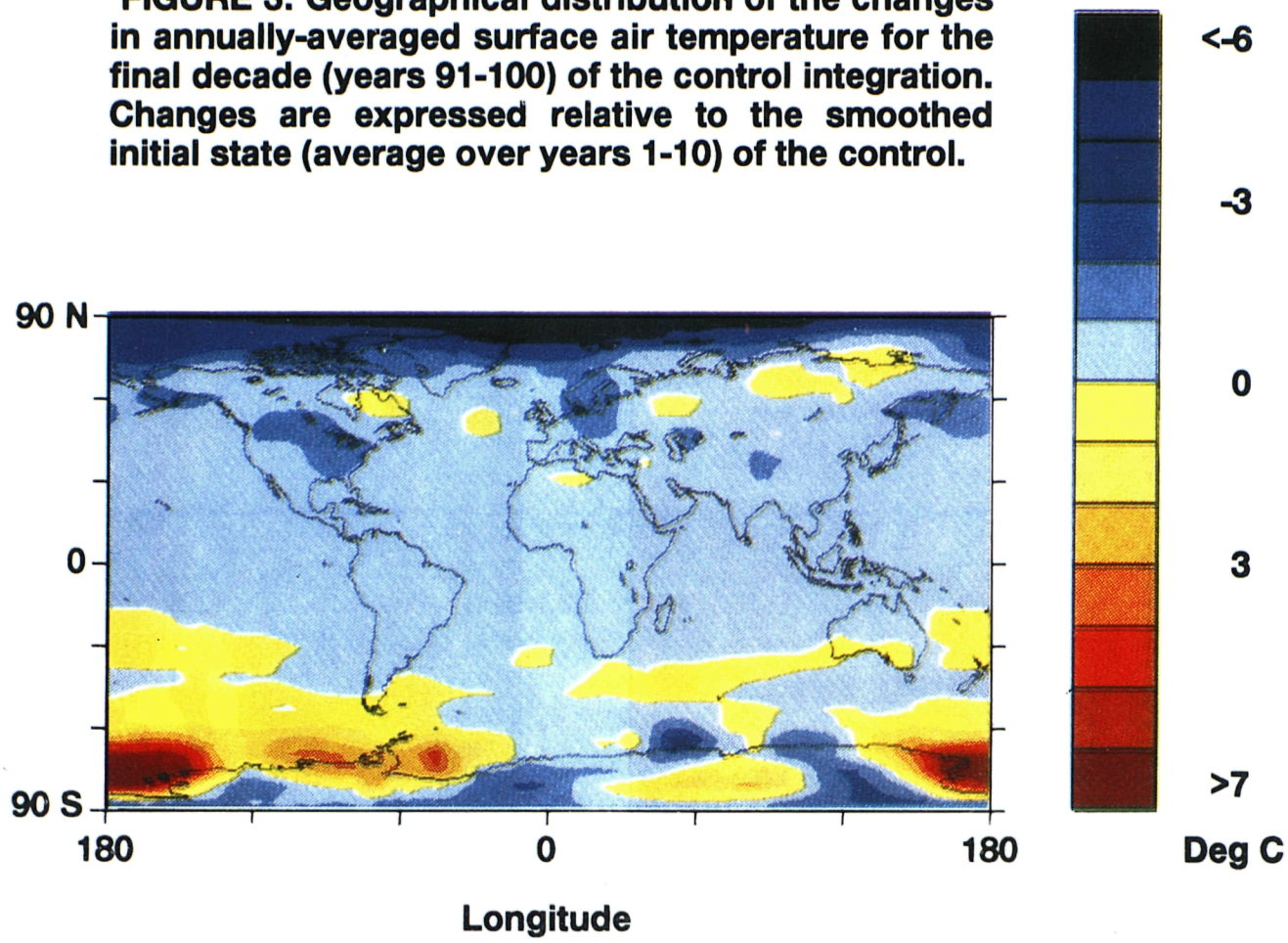

FIGURE 4: EOF 1 of the annually-averaged surface air temperature changes for Scenario A (a) and the control run (b). The explained variance is 84.1% and 52.5% respectively.

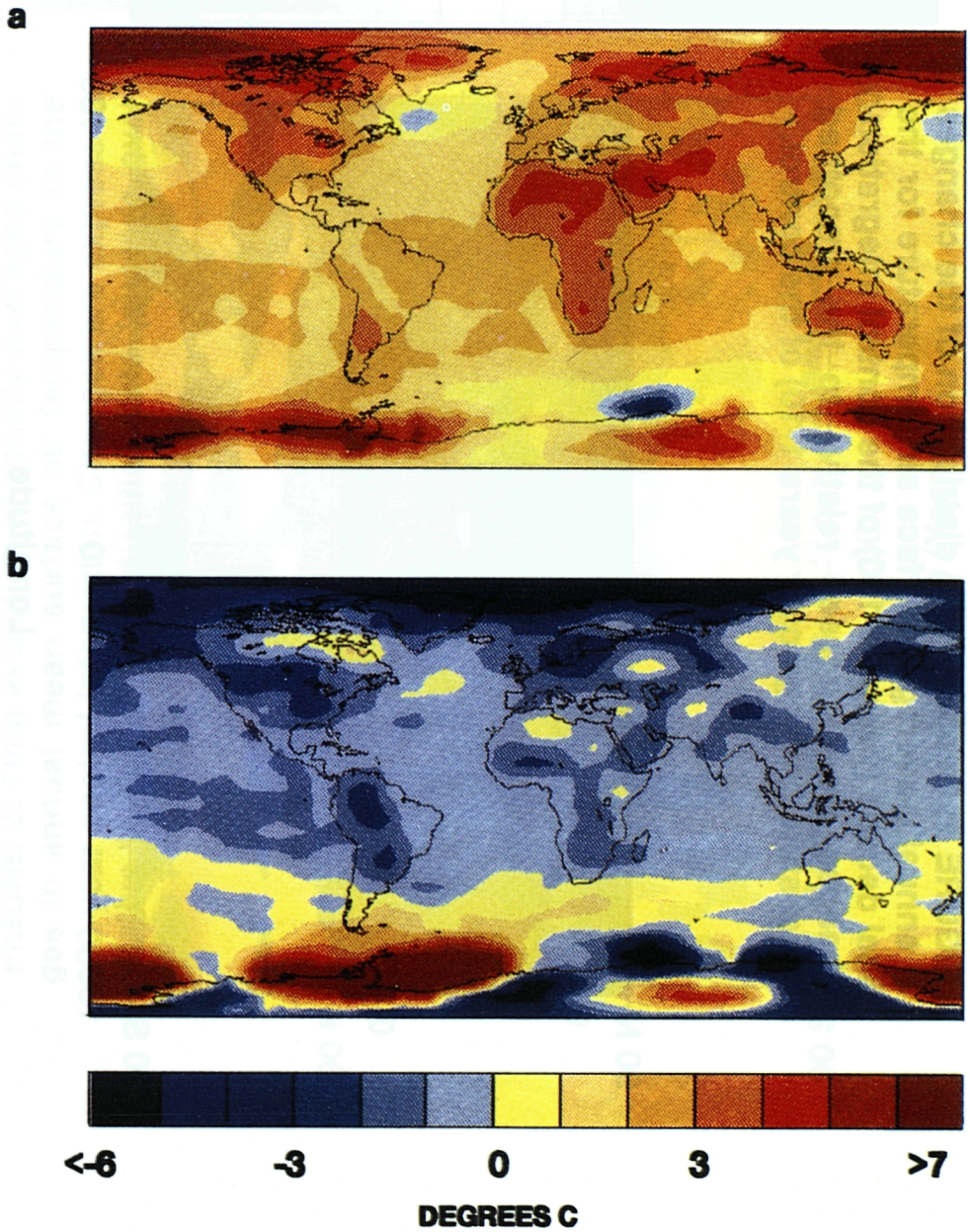

FIGURE 5: Principal component time series for the projection of the surface air temperature response fields of the three greenhouse warming experiments and the control run onto EOF 1 of Scenario A.

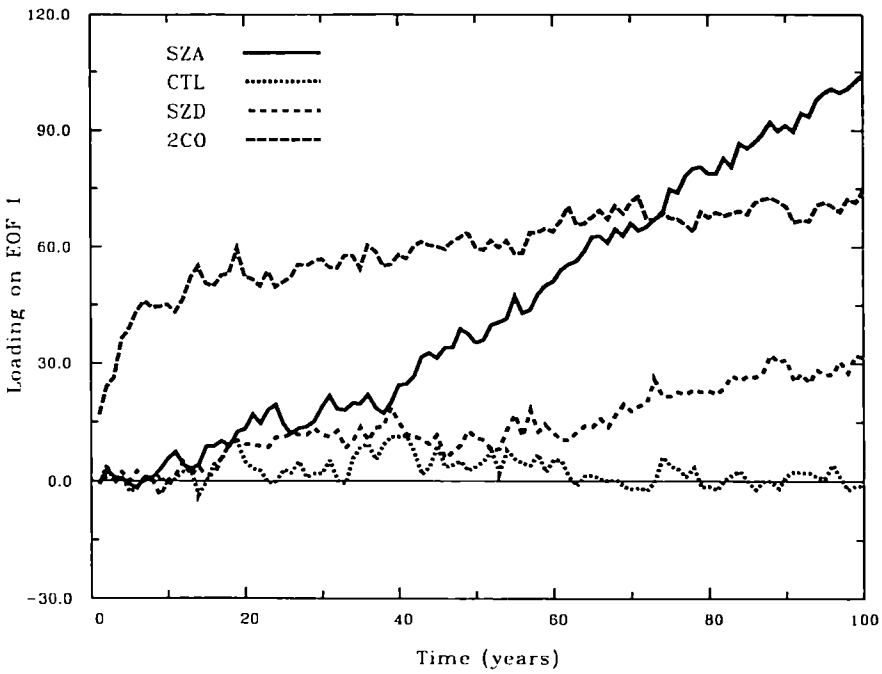

FIGURE 6: EOF 1 of the zonally-averaged annual mean temperature changes at 19 atmospheric levels for Scenario A (a) and the control run (b). The explained variance is 97.6 and 61.4% respectively

a

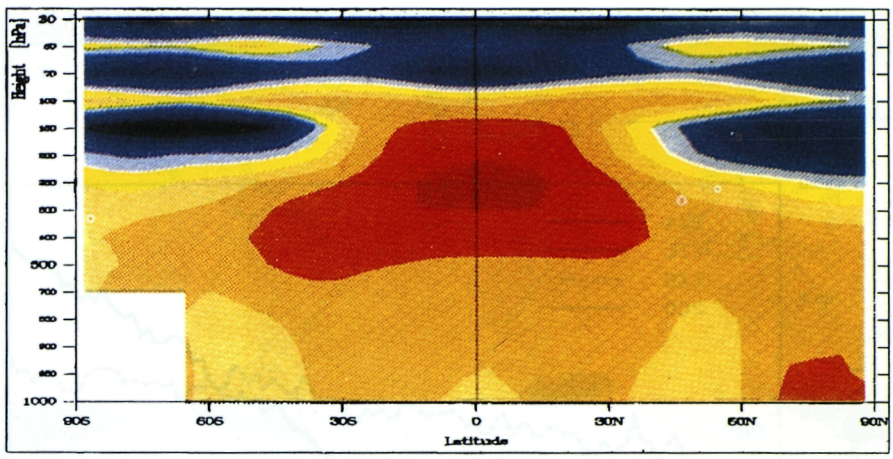

b

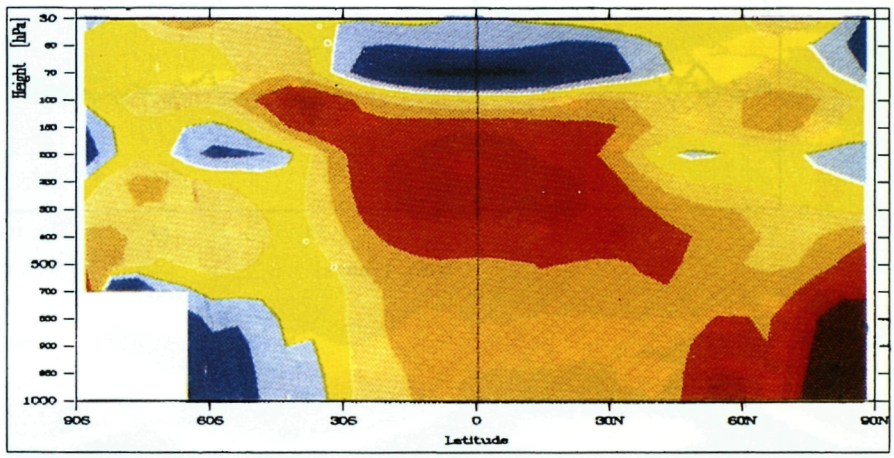

<-6 -3 0 3 >7

DEGREES C

FIGURE 7: Relationship between the linear trends in the Scenario A and control run PC 1 time series (see Figure 5) and the standard error *b*, a measure of the variance of linear trends (due to internally-generated natural variability) on the 100-year timescale. Results from a 3,800 year experiment with an uncoupled ocean model were used in order to estimate values of *b* for 21 globally- and regionally-averaged ocean variables.

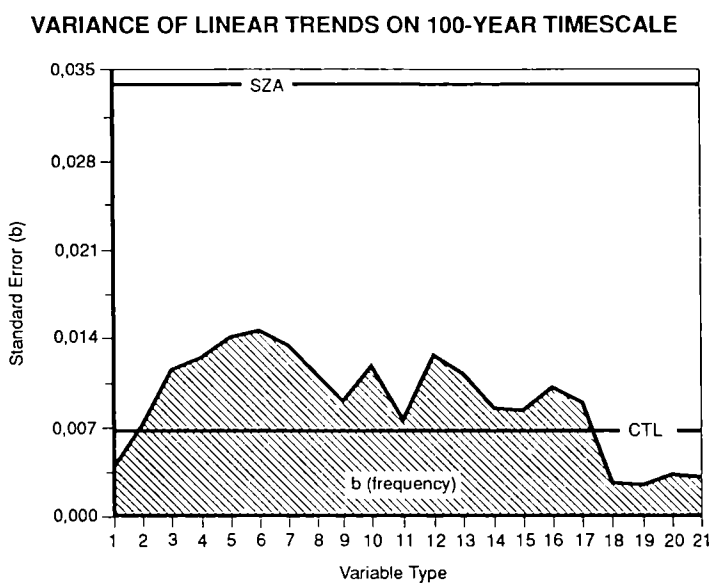

Variable Types

1 = Temperature 4000 m
2 = Salinity 4000 m
3 = Mass Transport, Drake Passage
4 = Ice Volume, North Atlantic
5 = Ice Volume, Antarctic
6 = Convection, North Atlantic
7 = Convection, Antarctic
8 = Heat Flux, North Atlantic
9 = Heat Flux, North Pacific
10 = Heat Flux, Antarctic
11 = Heat Flux, 30°N - 30°S
12 = Streamfunction 1500 m, Atlantic
13 = Streamfunction 2500 m, Atlantic
14 = Streamfunction 1500 m, Pacific
15 = Streamfunction 2500 m, Pacific
16 = Streamfunction 1500 m, Indian
17 = Streamfunction 2500 m, Indian
18 = Freshwater Flux, North Atlantic
19 = Freshwater Flux, North Pacific
20 = Freshwater Flux, Antarctic
21 = Freshwater Flux, 30°N - 30°S